Title
Construction and application of infectious citrus viroids for biological indexing

Journal
Journal of Citrus Pathology, 3(1)

Authors
Steyn, C
Cook, G
Burger, J T
et al.

Publication Date
2016

DOI
10.5070/C431037092

OPEN ACCESS Freely available online

Journal of Citrus Pathology

Research Article

Construction and application of infectious citrus viroids for biological indexing

C Steyn[1,2*], G Cook[1], JT Burger[2], and HJ Maree[2,3]

[1]Citrus Research International, P.O. Box 28, Nelspruit 1200, South Africa; [2]Department of Genetics, Stellenbosch University, Private Bag X1 Matieland, Stellenbosch 7602, South Africa; [3]Agricultural Research Council, Infruitec-Nietvoorbij (The Fruit, Vine and Wine Institute), Private Bag X5026, Stellenbosch7599, South Africa.

*Correspondence to: chanelsteyn1@gmail.com

Citation: Steyn C, Cook G, Burger JT, Maree HJ. 2016. Construction and application of infectious citrus viroids for biological indexing. J Cit Pathol. iocv_journalcitruspathology_37092.

Abstract

Viroid species identified in citrus induce a range of symptoms in this host as well as in non-citrus hosts. Currently, 7 citrus viroid species are recognized including *Citrus bent leaf viroid* (CBLVd), *Hop stunt viroid* (HSVd), *Citrus dwarfing viroid* (CDVd), *Citrus bark cracking viroid* (CBCVd), *Citrus viroid V* (CVd-V), *Citrus viroid VI* (CVd-VI) and *Citrus exocortis viroid* (CEVd). Cachexia-inducing variants of HSVd and CEVd, which causes exocortis, are considered severe pathogens of citrus, whereas other viroid species induce less severe symptoms such as stunting, either singly or in combination. Some viroid species, such as CDVd, have previously been used to deliberately induce stunting for high density planting of citrus, but studies on the effects of commercial orchards are limited. Research on the effect of viroid species requires the isolation of single viroid species. Biological isolation of single species from naturally infected citrus is challenging since viroids seldom occur as single infections and are often found in combination with various other pathogens. The production of single viroid species clones for *in vitro* transcription enables the generation of a single viroid species inoculum for research applications and circumvents the need for maintenance of sources in plants. Complete genomes of 7 viroid strains including CBLVd, 2 HSVd variants (CVd-IIa and CVd-IIb), CDVd, CBCVd, CVd-V and CEVd were cloned with a leading T7 promoter sequence to facilitate *in vitro* transcription. Circularized RNA transcripts were successfully used to transfect 'Etrog' citron (*Citrus medica*) by slash-inoculation that developed typical citrus viroid symptoms.

Keywords: Citrus viroids, *in vitro* transcription, slash-inoculation, infectious

Introduction

Viroids are small, circular, naked, single-stranded RNA molecules ranging from 240-400 nucleotides in length, lacking any protein coding ability. The high degree of base pair self-complementarity in their genomes promote stable secondary structures that have been shown to influence functionality (Flores et al. 2009). All citrus viroids belong to the *Pospiviroidae* family due to their secondary structure conformation, and characteristically have a rod-like structure with a central conserved region (CCR) that is mostly preserved among strains of a species (Flores et al. 2011; Di Serio et al. 2014). Further, specific domains are found, including the pathogenic (P) and variable (V) regions, located between the -left (T_L) and -right (T_R) termini and the CCR respectively, as illustrated in Fig. 1.

Seven citrus viroid species are currently recognized, namely *Citrus bent leaf viroid* (CBLVd), *Hop stunt viroid* (HSVd), *Citrus dwarfing viroid* (CDVd), *Citrus bark cracking viroid* (CBCVd), *Citrus viroid V* (CVd-V) *Citrus viroid VI* (CVd-VI) and *Citrus exocortis viroid* (CEVd). Each species consists of more than 1 variant, often varying in pathogenicity. HSVd distinctly consists of non-pathogenic (CVd-IIa) and cachexia-causing (CVd-IIb and CVd-IIc) variants (Reanwarakorn and Semancik 1998; Reanwarakorn and Semancik 1999; Palacio-Bielsa et al. 2004; Serra et al. 2008). The population structure of viroid variants has additionally been shown to be influenced by the citrus host (Bernad et al. 2009).

Fig. 1. Schematic representation of the rod-like secondary structure of the *Pospiviroidae* viroid family consisting of a central conserved region (CCR) and -left (T_L) and -right (T_R) termini flanking the pathogenic (P) and variable (V) domains (adapted from Serra et al. 2008).

Citrus viroids cause various symptoms in commercial citrus ranging from stunting, bark scaling, bark cracking, and pitting and gumming of the wood (Vernière et al.

2004). Symptomology can differ in severity depending on a number of factors including the sensitivity of the scion or rootstock, synergism in mixed infections, either with other viroids or other pathogens, and also environmental factors such as temperature (Duran-Vila et al. 1993; Vernière et al. 2006; Bernad et al. 2009; Serra et al. 2014). The spatial distribution of a viroid within a single plant can be erratic (Garnsey et al. 2002) and infection by multiple species can affect the titer of individual species (Barbosa et al. 2002). Given this complexity, a method to produce single viroid sources are required to enable the study of aspects such as symptom expression and synergistic interactions.

The most commonly used biological indicator host for citrus viroids is 'Etrog' citron, Arizona 861-S-1, (*Citrus medica*). Typical viroid symptoms on this host include leaf tip browning, petiole wrinkle and browning, mid-vein necrosis, leaf epinasty, leaf bending, bark cracking, gumming, and tree stunting (Duran-Vila et al. 1988). Symptom expression under optimal greenhouse conditions can be diagnostic for singly-infected plants, but overlapping symptoms do occur with some of the viroids, reducing the reliability of biological indexing for specific diagnostics (Duran-Vila et al. 1993). Moreover, it is also not possible to verify components of mixed infections biologically due to the synergistic effects between the viroids, affecting symptom expression (Vernière et al. 2006). A molecular diagnostic technique, in combination with biological indexing, is therefore required for definitive verification.

The use of viroid transcripts to infect plants has previously been demonstrated using various semi-*in vivo* and *in vitro* methods including the use of viroid complementary DNA (cDNA), recombinant plasmid DNA (pDNA) (Visvader et al. 1985; Hajeri et al. 2011) and *in vitro*-synthesized linear and circularized RNA transcripts (Rezaian 1999; Serra et al. 2008). Following inoculation, various host enzymes and replication mechanisms are utilized to amplify viroid RNA, allowing systemic spread and viroid infection (Flores et al. 2008). Infectivity of circularized transcripts has previously been shown to be more effective than linear transcripts (Rezaian 1999).

In this study, full-length viroid sequences were first determined from infected plants and the information used to construct clones containing the universal T7 promoter directly preceding the viroid sequence. Full-length viroid RNA was transcribed and enzymatically circularized before slash inoculation of 'Etrog' plants that developed typical citrus viroid symptoms corresponding to the inoculated viroid RNA species. Traditional biological indexing protocols for citrus viroids require the use of *in planta* maintained citrus viroid positive controls. However, such controls may harbor other pathogens or a mixture of viroid species. Maintenance of these plants also requires a significant investment of time, labor and greenhouse space – resources that may not be available to all citrus programs. We propose that the protocol developed in this study can be an alternative to the use of *in planta* maintained citrus viroid controls for routine biological indexing.

Materials and Methods

Viroid sources

The following viroid species were used for the construction of infectious clones: CBLVd, 2 HSVd variants (CVd-IIa and CVd-IIb), CDVd, CBCVd, CVd-V and CEVd. RNA sources were all field derived and, in most cases, contained multiple viroid species per sample. Total RNA was extracted from petioles and leaf mid-ribs using an acid-phenol extraction protocol (Cook et al. 2015).

Strain isolation

Based on the minimum free energy, the secondary structure for each viroid species was determined from a consensus sequence generated in CLC Sequence Viewer 7 using sequences downloaded from the NCBI database. Structures were determined using Mfold (http://unafold.rna.albany.edu/?q=mfold/rna-folding-form) with standard parameters set for circular sequences. The CCR was identified for each viroid and adjacent species-specific conserved region (CR)-primer sets (Table 1) were designed using OligoExplorer (http://www.genelink.com/tools/gl-oe.asp) for amplification of full genomes.

RT-PCR was performed for each viroid using the CR-primer sets (Table 1) and RNA obtained from various field sources. Complementary DNA (cDNA) was synthesized by denaturation of 0.5-1 µg total RNA together with 0.1 µM CR-reverse primer in a 10 µl reaction volume for 3 min at 65°C, followed by 1 min incubation on ice. Thereafter, reverse transcription reagents were added, including 40 U RevertAid H Minus Reverse Transcriptase (Thermo Fisher Scientific), 10 U Ribolock RNAse Inhibitor (Thermo Fisher Scientific) and 1 mM of each dNTP (Thermo Fisher Scientific) in a total volume of 20 µl. These reactions were incubated at 50°C for 60 min, followed by an enzyme deactivation for 5 min at 85°C. PCR was performed using 2 µl cDNA with 0.5 U Phusion® High Fidelity DNA polymerase (New England BioLabs, USA), 0.2 mM dNTPs (each) and 0.5 µM of each primer (CR-forward and -reverse) in 25 µl total volume reactions, following the cycling profile: 98°C for 2 min and 35 cycles of 98°C for 10 sec, specific annealing temperature (Table 1) for 30 sec and 72°C for 20 sec, with a final extension at 72°C for 5 min. PCR products were gel-purified using the Zymoclean™ gel DNA Recovery kit (Zymo Research, CA, USA) and bi-directionally sequenced using the CR-primer sets.

Cloning and transcription template construction

Adjacent terminal region (TR-) primer sets were designed from the genome sequences generated and presented in Table 2. A T7 promoter sequence was added to the 5'-end of each forward primer. Either the T_L- or T_R-region was targeted to avoid the high degree of base-pair complementarity in the stem regions. The first viroid nucleotide following the T7 promoter sequence was selected to be a guanine base, which is required for the initiation of transcription for T7 RNA Polymerase.

Table 1
Conserved region primer sequences for each viroid, the annealing temperatures used and expected amplicon sizes. The GenBank sequence accession numbers for the full-genomes of each viroid are also presented.

Viroid	Primers	Sequence (5' to 3')	Annealing Temperature (°C)	Product Size (bp)	Annealing Sites	GenBank Accession
CBLVd[a]	Forward	AAGCCCCGTGAACCCCTGAG	57	327	302-321	KY110715
	Reverse	CACCCTCTCCCCGCTGCTAC			301-282	
HSVd (CVd-IIa)[b]	Forward	TTTTACCTTCTCCTGGCTCTTCG	52	300	185-207	KY110716
	Reverse	GAAGAAGGGACGATCGATGGT			184-164	
HSVd (CVd-IIb)[b]	Forward	GAATCCAGCGGGGGCGTGGAG	60	300	99-119	KY110717
	Reverse	TGAGAAGAGTTGCCCCGGGG			98-79	
CDVd[c]	Forward	CGAAGGCAGCTAAGTTGGTGA	58	295	92-112	KY110718
	Reverse	TCGACGACGACAGGTAAGTT			91-72	
CBCVd[d]	Forward	GGTGGATACAACTCTTGGG	51	284	217-235	KY110719
	Reverse	GGGTAGTTTCTATCTCAGGTC			216-196	
CVd-V[e]	Forward	CACGATTGGTGTTCTCCC	52	299	227-294	KY110720
	Reverse	TTTTACCCTGGGGACACC			226-209	
CEVd[f]	Forward	GGAAACCTGGAGGAAGTCGA	53	372	99-118	KY110721
	Reverse	CCGGGGATCCCTGAAGGA			98-81	

[a] *Citrus bent leaf viroid*, [b] *Hop stunt viroid*, [c] *Citrus dwarfing viroid*, [d] *Citrus bark cracking viroid*, [e] *Citrus viroid V*, [f] *Citrus exocortis viroid.*

Table 2
Terminal region viroid-specific primer sequences including the additional T7 promoter sequence (underlined) added to the forward primer. Annealing temperatures, specific annealing sites on the viroid genomes and expected product sizes are presented.

Viroid	Primers	Sequence (5' to 3')	Annealing Temperature (°C)	Product Size (bp)	Annealing Sites
CBLVd[a]	Forward	TGTAATACGACTCACTATAGGAGACTTCTTGTGGTTCCTGTGGTG	66	346	2-27
	Reverse	GAGGAGCCCTCAGGGGTTCAGG			1-305
HSVd[b] variants	Forward	TGTAATACGACTCACTATAGGGGAATTCTCGAGTTGCCGCAT	65	319	3-25
	Reverse	AGAGGGGCTCAAGAGAGGATCCG			2-280
CDVd[c]	Forward	TGTAATACGACTCACTATAGAAACTCCGTGTGGTTCCTGTGGGG	65	314	5-29
	Reverse	CTCCGGGGAAACACCAATCGTGT			4-275
CBCVd[d]	Forward	TAATACGACTCACTATAGGGAATTTCTCTGCG	63	301	4-18
	Reverse	CAGAGGGGTCTCAAACGCGGGCCAT			3-265
CVd-V[e]	Forward	TGTAATACGACTCACTATAGTCACCCCGCCCCACGGGAAATAAAA	70	313	29-54
	Reverse	CCACAGGAACCACAAGGTTGTTCACC			28-3
CEVd[f]	Forward	TGTAATACGACTCACTATAGATCACTGGCGTCCAGCGGAGAAACA	71	391	151-176
	Reverse	CGCGGCGACCGAAGCTGTTGA			150-130

[a] *Citrus bent leaf viroid*, [b] *Hop stunt viroid*, [c] *Citrus dwarfing viroid*, [d] *Citrus bark cracking viroid*, [e] *Citrus viroid V*, [f] *Citrus exocortis viroid.*

The terminal hairpins of the T_L-regions of HSVd variants are conserved and the same the TR-T7-primers were used to amplify both HSVd variants (CVd-IIa and CVd-IIb). Complementary DNA synthesis and PCRs were performed using the same RNA sources as above, but using the TR-T7-primer sets and specific annealing temperatures as listed in Table 2.

RT-PCR products generated using the TR-T7-primers were gel purified as described above. These amplicons were cloned into pGEM-T Easy vector via TA-cloning as per supplier's protocol (Promega). The ligated plasmids were transformed into competent DH5α E. coli cells which were then plated onto Luria Broth agar plates containing 100 µg/ml Ampicillin, 40 µg/ml X-gal and 0.2 mM IPTG for blue/white selection of recombinants. Plates were incubated overnight at 37°C.

Ten white colonies for each viroid variant were selected and tested by PCR for inserts with the correct orientation. Sterile pipette tips were used to pick cells from each selected white colony which were resuspended in PCR reaction mixes containing: 0.4 µM universal T7 promoter primer (5'-TAATACGACTCACTATAGGG-3'), 0.4 µM of the corresponding TR-T7-forward primer and GoTaq G2 Hot Start Green MasterMix (Promega) in 10 µl total volume reactions. Samples yielding products of the correct size indicated plasmids with viroid inserts in the correct orientation. Recombinant plasmids were extracted using the GeneJET Plasmid Miniprep kit (Thermo Fisher Scientific). The complete sequences of the inserts were determined by Sanger sequencing using the universal SP6-promoter primer. Using CLC Sequence Viewer 7, these sequences were compared to the initial sequences obtained from the amplification products using the CR-primer sets. This was done to confirm that no nucleotide misincorporations had occurred during the RT-PCR and cloning processes. These confirmed sequences were submitted to GenBank and the accession numbers are presented in Table 1. A single clone of each viroid species was used for downstream analyses.

In vitro transcription template and inoculum preparation

The recombinant plasmids were used to produce full-length viroid double-stranded template DNA which included the T7 promoter required for transcription. PCR amplifications were performed using Kapa HiFi HotStart ReadyMix (Kapa Biosystems) and 0.3 µM of each TR-T7-primer (Table 2). Amplicons were gel purified as before. The HiScribe T7 High Yield RNA synthesis kit (New England BioLabs) was used for *in vitro* transcription using the purified dsDNA template. The prescribed protocol for short RNA transcripts (<0.3 kb) was followed, using approximately 300 ng of template DNA, 7.5 mM of each NTP (A, U, G, C) and 1.5 µl T7 RNA Polymerase mix in 20 µl reaction volumes and incubated at 37°C for 3 hours. RNA transcripts were purified by phenol-chloroform extractions and ethanol precipitation steps, and resuspended in 200 µl nuclease-free water. Approximately 6 µg full-length viroid ssRNA transcripts were dephosphorylated with 10 U Calf Intestinal Alkaline Phosphatase (New England BioLabs) in 20 µl total volume reactions for 30 min at 37°C. After phenol-chloroform purification and ethanol precipitation, RNA was resuspended in 15 µl nuclease-free water. Monophosphorylation was performed by adding 10 U T4 polynucleotide kinase (New England BioLabs) and 1 mM ATP to 13 µl dephosphorylated RNA in 50 µl total volume reactions and incubated at 37°C for 30 min followed by 10 min at 65°C. Viroid circularization was completed by adding 10 U T4 ssRNA Ligase 1 (New England BioLabs) and incubation at 37°C for 15 min. To assess that circularization had occurred, RT-PCRs were performed using the CR-primer sets spanning the ligation junctions. Both linear and circularized transcripts were diluted to 2 ng/µl in 20 mM NaH_2PO_4 buffer for inoculation.

Slash-inoculation and transfection

Twelve-month-old 'Etrog' seedlings were slash-inoculated 30-40 cm from the plant base. A 5 µl droplet of the prepared inoculum was pipetted onto the stem just below a bud and slashed through 4-6 times into the phloem with a sterile scalpel blade (Fig. 2 A-C). The slash sites were sealed with parafilm to prevent desiccation. For each viroid, 9 seedlings were slash-inoculated with circularized transcripts, and 3 with linear transcripts, as well as 1 plant for each of the following controls: No transcription-enzyme control, NaH_2PO_4-buffer control and No-inoculum control.

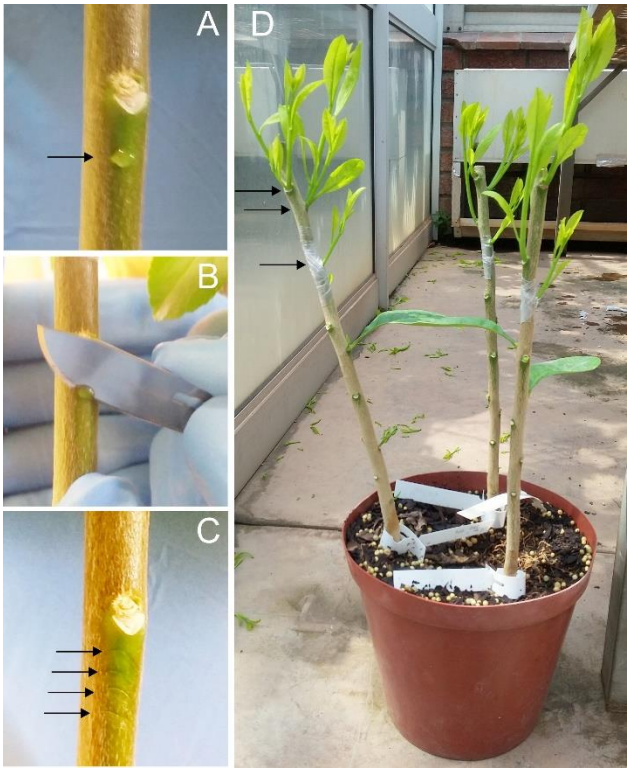

Fig. 2. Slash-inoculation and cut-back procedures. (A) 5 µl inoculum droplet pipetted just beneath bud; (B) Slashing through droplet with sterile scalpel blade; (C) Four horizontally slanted slashes into phloem tissue beneath the bud; (D) Cut-back shoots with new growth from all 3 buds left above slash site, 2 weeks post-inoculation.

For the first week post-inoculation (PI), the plants were maintained in a glasshouse compartment maintained at 24-28°C to avoid undue plant stress. Thereafter, all plants were cut back at 3 buds above the slash site (Fig. 2D), and transferred to a warmer compartment with temperatures maintained at 28-32°C to encourage plant growth and viroid symptom expression (Duran-Vila et al. 1993).

One month PI, 2 leaves were sampled from each plant. Total RNA extraction was performed as before and RT-PCR done using the CR-primer sets to confirm viroid transmission. All plants were tested for the full complement of viroids to confirm single infections. DNA amplicons were bi-directionally sequenced to compare the viroid sequences with original input sequences. Sequences were aligned in CLC Sequence Viewer 7, point mutations identified and their nucleotide position on the viroid genomes determined. An overview of the entire experimental approach is illustrated in Fig. 3.

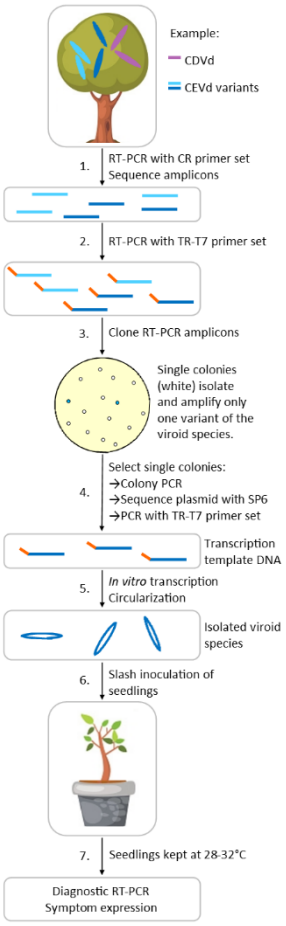

Fig. 3. Overview of infectious viroid construction and transfection. (1) Viroid species sequence determination using CR-primers; (2) Full-genome amplification containing additional T7 promoter sequence; (3) Cloning of amplicons including the T7 promoter; (4) Sequence confirmation using universal SP6 primer. Preparation of transcription templates using TR-T7-primers; (5) *In vitro* transcription and circularization; (6) Slash-inoculation to 'Etrog' citron seedlings; (7) Seedlings kept at 28-32°C before transfection confirmation (RT-PCR using CR-primers) and symptom evaluation.

Results

In vitro transcription

Visualization of the linear RNA transcripts on a TAE-agarose gel, following *in vitro* transcription from PCR-generated dsDNA templates, showed that each viroid transcript appeared smaller than the DNA template. Input DNA template of the expected size for CEVd can be seen in the 'no-enzyme' control lane (Fig. 4). The intensities of the bands of the various viroid transcripts differed visually, even though equivalent template DNA amounts were used for transcription (Fig. 4). The transcripts produced for CDVd and CEVd were noticeably less than for the other viroids, and bands for HSVd variants and CBCVd were more prominent. Circularized RNA transcripts were similarly run on agarose gels and the same rapid mobility of transcripts was observed due to the secondary structure formations. Only the first figure is presented as no difference was observed between the linear and circularized forms.

Transfection and symptomology

Successful transmission of all the circularized viroid transcripts was confirmed by RT-PCR. No infection was observed when linear transcripts were used to transfect the plants. Viroid sequences obtained from the positively transfected plants were compared to the viroid sequences of the original sources using CLC Sequence Viewer 7. No mutations that might have been introduced during cloning, *in vitro* transcription and *in planta* replication for all the viroids apart from CEVd were detected. Three point mutations were identified in the CEVd genome at positions C232U, A234G and U314A (GenBank accession: KY110722). Additionally, the original CEVd variant was also present in the plant. In the Sanger sequence electropherogram, both variant bases were visible as fluorescent peaks at each of the mutation points.

Two months PI, some typical viroid symptoms were visible on the 'Etrog' host. The symptoms observed are presented in Table 3 and Fig. 5. CBCVd and CEVd infected plants however, only showed typical symptoms 14 months PI, despite positive transmission being confirmed one month PI.

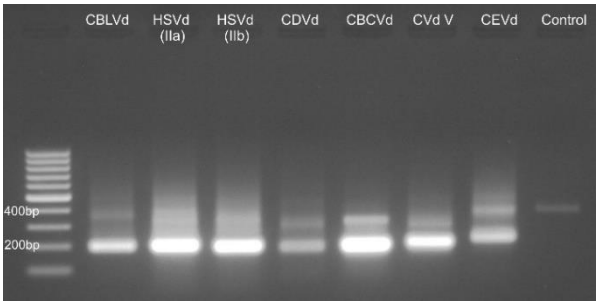

Fig. 4. A 1.5% TAE-agarose gel showing the viroid RNA transcripts. Lanes after a 100 bp DNA marker (Thermo Fisher Scientific) contain RNA transcripts *Citrus bent leaf viroid*, *Hop stunt viroid* (CVd-IIa), *Hop stunt viroid* (CVd-IIb), *Citrus dwarfing viroid*, *Citrus bark cracking viroid*, *Citrus viroid V*, *Citrus exocortis viroid* and No-T7 RNA Polymerase enzyme control with CEVd dsDNA as template.

Table 3
Symptoms observed on 'Etrog' after transfection with circularized viroid RNA transcripts. The presence of symptoms is indicated by +. The alphabet letters after the symptom description relate to photographs in Fig. 5 depicting these symptoms.

Viroid	Leafbend (A)	Leaf drooping (B)	Leaf tip browning (C)	Mid-vein necrosis (D)	Stunting/ Dwarfing (E)	Bark cracking (F)	Gumming (G)	Petiole browning (H)	Petiole wrinkle (I)	Epinasty (J)
CBLVd[a]	+			+						
HSVd (CVd-IIa)[b]			+							
HSVd (CVd-IIb)[b]			+	+						
CDVd[c]		+			+			+	+	
CBCVd[d]				+		+	+	+		
CVd-V[e]	+							+		
CEVd[f]										+

[a] *Citrus bent leaf viroid,* [b] *Hop stunt viroid,* [c] *Citrus dwarfing viroid,* [d] *Citrus bark cracking viroid,* [e] *Citrus viroid V,* [f] *Citrus exocortis viroid.*

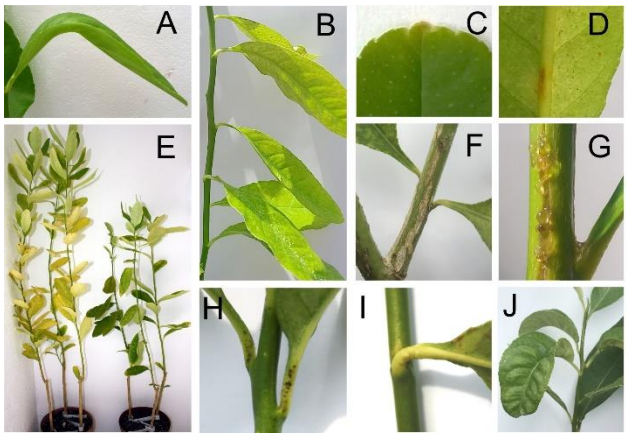

Fig. 5. Typical symptoms on 'Etrog' citron. (A) Leaf bend; (B) Leaf drooping; (C) Leaf tip browning; (D) Mid-vein necrosis; (E) Stunting/Dwarfing; (F) Bark cracking; (G) Gumming; (H) Petiole browning; (I) Petiole wrinkle; and (J) Epinasty.

Discussion

Seven citrus viroids were successfully cloned with a leading T7 transcription promoter and the clones used to transfect 'Etrog' seedlings. The complete genome of each viroid was determined by targeting the conserved regions of each viroid species for amplification and sequencing the variable terminal region. Primers were then designed in the terminal region to allow for the amplification of complete viroids with the addition of a T7 promoter for subsequent *in vitro* transcription.

Upon *in vitro* transcription, the ssRNA transcripts formed secondary structure conformations which were observed by the faster movement of the transcripts through the agarose gel, compared to linear dsDNA templates as was also observed for the transcripts after circularization reactions. Although RT-PCRs were performed to assess that circularization had occurred, this could not verify the efficiency of circularization. It was also noted that the band intensity of transcripts of the viroid species differed (Fig. 4) and correlated with the number of guanine nucleotides after the T7 promoter sequence. A guanine nucleotide after the T7 promoter is essential for successful transcription initiation (Milligan et al. 1987) and transcription yield has been shown to increase with an increase of purine bases at the initiation site following the T7 promoter sequence (Moll et al. 2004; Imburgio et al. 2000).

Transfection of the 'Etrog' host with each of the 7 circularized viroid species was confirmed 1 month PI. Although the primary objective was not to compare the infectivity of linear to circularized transcripts, no transmission was detected when inoculating with linear transcripts. Fewer plants were however inoculated with linear compared to circularized transcripts and this possibly limited the potential to obtain transmission using linear transcripts. A previous study found that transmission using linear RNA transcripts was less effective than using circularized viroids (Rezaian 1999).

Despite the early molecular detection of CEVd in the host, mild epinasty was only observed more than 1 year PI. Although the original variant was present in the plant, another mutated variant was also detected. Three point mutations were identified from the original sequence; 2 within the variable region (C232U, A234G) and 1 within the pathogenic region (U314A). Variants of CEVd have previously been characterized (Bernad et al. 2009; Hajeri et al. 2011) and Bernard et al. (2009) showed that the variant population in the original citrus host changed when introduced to other citrus types including 'Etrog'. We suspect therefore that the point mutations in the CEVd genome observed in this study, might have been host induced. Mutations within the pathogenic region have been studied extensively and are known to alter the symptom expression. Murcia et al. (2011) investigated two point mutations at position 314 and 315 within the pathogenic region, and found that mutations at these points resulted in a variant of CEVd that caused no symptom expression on 'Etrog'. The point mutation at position 314 within the pathogenic region as found in this study, can therefore explain the reduced symptom expression observed.

This cloning and transcription process produced single viroid sources of CBLVd, non-pathogenic HSVd (CVd-IIa), cachexia-causing HSVd (CVd-IIb), CDVd, CBCVd,

CVd-V and CEVd, a resource for future viroid studies and use in routine biological indexing protocols. The recombinant plasmid DNA containing full-viroid genome inserts can be stored long term with greater ease and most likely lower cost than maintaining viroid sources *in planta*.

Acknowledgments

We thank Kobus Breytenbach for his assistance with the inoculation and maintenance of the plants, and Dr. Fanie van Vuuren for his willing advice and inputs. We acknowledge Citrus Research International and The Technology and Human Resources for Industry Programme for funding the project.

References

Barbosa CJ, Pina JA, Navarro L, Duran-Vila N. 2002. Replication/accumulation and symptom expression of citrus viroids on some species of citrus and related genera. Fifteenth IOCV Conf. 15:264–271.

Bernad L, Duran-Vila N, Elena SF. 2009. Effect of citrus hosts on generation, maintenance and evolutionary fate of genetic variability of citrus exocortis viroid. J Gen Virol. 90:2040–2049.

Cook G, van Vuuren SP, Breytenbach JHJ, Burger J, Maree H. 2015. Expanded strain-specific RT-PCR assay for differential detection of currently known citrus tristeza virus strains: a useful screening tool. Phytopathology. 164:847–851.

Di Serio F, Flores R, Verhoeven JT, Li SF, Pallás V, Randles JW, Sano T, Vidalakis G, Owens RA. 2014. Current status of viroid taxonomy. Arch Virol. 159:3467–3478.

Duran-Vila N, Pina JA, Navarro L. 1993. Improved indexing of citrus viroids. Twelfth IOCV Conf. 12:202–211.

Duran-Vila N, Roistacher CN, Rivera-Bustamante R, Semancik JS. 1988. A definition of citrus viroid groups and their relationship to the exocortis disease. J Gen Virol. 69:3069–3080.

Flores R, Carbonell A, Gago S, de Alba AM, Delgado S, Rodio M, Di Serio F. 2008. Viroid-host interactions: a molecular dialogue between two uneven partners. Biol plant-microbe Interact. 6:1–9.

Flores R, Gas ME, Molina-Serrano D, Nohales MÁ, Carbonell A, Gago S, de la Peña M, Daròs J. 2009. Viroid replication: rolling-circles, enzymes and ribozymes. Viruses. 1:317–334.

Flores R, Grubb D, Elleuch A, Nohales MÁ, and Delgado S. 2011. Rolling-circle replication of viroids, viroid-like satellite RNAs and hepatitis delta virus: variations on a theme. RNA Bio. 8(2):200–6.

Garnsey SM, Zies DL, Irey M, Sieburth PJ, Semancik JS, Levy L, Hilf M. 2002. Practical field detection of citrus viroids in Florida by RT-PCR. Fifteenth IOCV Conf. 15:219–229.

Hajeri S, Ramadugu C, Manjunath K, Ng J, Lee R, Vidalakis G. 2011. *In vivo* generated citrus exocortis viroid progeny variants display a range of phenotypes with altered levels of replication, systemic accumulation and pathogenicity. Virology. 417:400–409.

Imburgio D, Rong M, Ma K, McAllister WT. 2000. Studies of promoter recognition and start site selection by T7 RNA polymerase using a comprehensive collection of promoter variants. Biochemistry. 39:10419–10430.

Milligan JF, Groebe DR, Witherell GW, Uhlenbeck OC. 1987. Oligoribonucleotide synthesis using T7 RNA polymerase and synthetic DNA templates. Nucleic Acids Res. 15:8783–98.

Moll PR, Duschl J, Richter K. 2004. Optimized RNA amplification using T7-RNA-polymerase based *in vitro* transcription. Anal Biochem. 334:164–174.

Murcia N, Bernad L, Duran-Vila N, Serra P. 2011. Two nucleotide positions in the citrus exocortis viroid RNA associated with symptom expression in Etrog citron but not in experimental herbaceous hosts. Mol Plant Pathol. 12:203–208.

Palacio-Bielsa A, Romero-Durbán J, Duran-Vila N. 2004. Characterization of citrus HSVd isolates. Arch Virol. 149:537–552.

Reanwarakorn K, Semancik JS. 1998. Regulation of pathogenicity in hop stunt viroid-related group II citrus viroids. J Gen Virol. 79:3163–3171.

Reanwarakorn K, Semancik JS. 1999. Correlation of hop stunt viroid variants to cachexia and xyloporosis disease of citrus. Phytopathology. 89:568–574.

Rezaian MA. 1999. Synthesis of infectious viroids and other circular RNAs. Curr Issues Mol Biol. 1:13–20.

Serra P, Bani-Hashemian SM, Fagoaga C, Romero J, Ruiz-Ruiz S, Gorris MT, Bertolini E, Duran-Vila N. 2014. Virus-viroid interactions: citrus tristeza virus enhances the accumulation of citrus dwarfing viroid in Mexican lime via virus-encoded silencing suppressors. J Virol. 88:1394–1397.

Serra P, Gago S, Duran-Vila N. 2008. A single nucleotide change in Hop stunt viroid modulates citrus cachexia symptoms. Virus Res. 138:130–134.

Vernière C, Perrier X, Dubois C, Dubois A, Botella L, Chabrier C, Bové JM, Duran-Vila N. 2004. Citrus viroids: symptom expression and effect on vegetative growth and yield of clementine trees grafted on trifoliate orange. Plant Dis. 88:1189–1197.

Vernière C, Perrier X, Dubois C, Dubois A, Botella L, Chabrier C, Bové JM, Duran-Vila N. 2006. Interactions between citrus viroids affect symptom expression and field performance of clementine trees grafted on trifoliate orange. Phytopathology. 96:356–368.

Visvader JE, Forster AC, Symons RH. 1985. Infectivity and *in vitro* mutagenesis of monomeric cDNA clones of citrus exocortis viroid indicates the site of processing of viroid precursors. Nucleic Acids Res. 13:5843–5856.